PHYSICAL REVIEW B VOLUME 27, NUMBER 12 15 JUNE 1983

Correlated random walk on lattices. II. Tracer diffusion through a two-component dynamic background

R. A. Tahir-Kheli
Department of Physics, Temple University, Philadelphia, Pennsylvania 19122
(Received 27 December 1982)

A detailed calculation of frequency- and wave-vector-dependent correlation functions for an arbitrary tracer diffusing in a regular crystal against a background of hopping classical particles has recently been given by Tahir-Kheli and Elliott [Phys. Rev. B 27, 844 (1983)]. Here we present an important generalization of this work to a system with a dynamic background consisting of *two* arbitrary species of particles. In particular, the generalization includes a system where the tracer concentration itself is finite while an arbitrary concentration of other atoms is also present in the dynamic stream. The theory is exact to the leading nontrivial order in particle concentration x_A and x_B. In the intermediate-concentration regime, the theory incorporates dominant fluctuations from the mean field. The present model can serve to usefully describe incoherent neutron scattering in metal-hydride interstitial solutions such as $MA_{x_A}B_{x_B}$ with $A,B \equiv$H, D, and T and $M \equiv$Pd and Ti. Moreover, it can be used to treat tracer diffusion dynamics in nonstoichiometric metal oxides and, somewhat more simplistically, ionic conduction in the superionic state.

I. INTRODUCTION

The dynamical, space-dependent self-correlation of a classical tracer, diffusing through a background of hopping atoms, is materially affected by the memory effects that result from the exclusion of double occupancy.[1] Despite the presence of the usual ingredients necessary for obtaining uncorrelated random-walk motion (namely, the stochasticity of the allowed hops and the absence of interparticle interactions), the stricture against multiple occupancy adds nontrivial complexity to the problem. Indeed, it causes strong correlations to occur between successive tracer jumps[2–4]—correlations that are reflected in the behavior of the tracer occupancy even at distances and times that are large on the scale specified by an elementary hop.

In a recent paper[1] [henceforth to be referred to as I and its equations as I(3.11), etc.] a detailed calculation of the tracer correlation function was given. An important asset of this work was its generality whereby the tracer and the background atom hopping rates, J^0 and J, were kept arbitrary. However, for certain physical applications, such as incoherent neutron scattering from a metal hydride with an interstitially dissolved mixture of hydrogen isotopes (e.g., H, D, and T where at least two species of hydrogen atoms have finite concentrations) the treatment given in I is inadequate.

The reason is the following. For the treatment given in I to be valid, either the concentration of tracer atoms (with hopping rate J^0) must be vanishingly small (i.e., there is only a single tracer in a crystal with N sites) or, if the tracer concentration is finite, then the tracer has to be identical to the background atoms (i.e., $J^0=J$, where J is the hopping rate of the background atoms).

To rectify this shortcoming, we present a generalization of the theory given in I so that it applies to the case where the labeled atom (with hopping rate J^0) diffuses against a background of *two* varieties of hopping atoms (with hopping rates J^A and J^B). For convenience of presentation, we again assume the concentration of tracer atoms to be vanishing. However, because J^0 like J^A and J^B is arbitrary, when $J^0=J^A$, for example, we obtain a binary mixture where the labeled atom belongs to species A with concentration x_A. Any further generalization, wherein the background consists of three or more species, A, B, C, etc., can be achieved straightforwardly along the present lines.

In this context it should be mentioned that the general case of a random A-B alloy with vacancies has already received some attention in the literature. Beginning with the work of Manning,[4] De Bruin *et al.*[5] and Murch and Rothman[6] have investigated tracer diffusion in such an alloy (the tracer being either atom A or B). However, their work is not only restricted to zero frequency and vanishingly small wave vectors; it also refers to the very specific limit

of zero vacancy concentration. Some preliminary analyses of the more general case with arbitrary vacancies have recently been reported by Fukai and collaborators[7] and Kutner and Kehr,[8] who have employed numerical simulations for this purpose.

II. EQUATIONS OF MOTION

We make the usual simplifying assumptions[8–17] regarding the instantaneous nature of the hops, allowed only across nearest-neighbor separation, and their stochasticity. Accordingly, the relevant rate equations for the stochastic occupancy variables of the tracer, $p_i(t)$, and the host atoms, $n_j^{\mu}(t)$ with $\mu \equiv A$ or B, are the following:

$$\frac{d\sigma_i}{dt} = -\sum_j J_{ij}^{\sigma}(\sigma_i V_j - \sigma_j V_i) , \tag{2.1}$$

where $\sigma_i \equiv p_i$, n_i^A, or n_i^B as the superscript $\sigma \equiv 0$, A, or B and

$$V_i = (1 - p_i - n_i^A - n_i^B) . \tag{2.2}$$

The variable $V_i(t)$ specifies the stochastic occupation variable for a vacancy to be present at the lattice position i at time t. When $0 = p_i(t) = n_i^A(t) = n_i^B(t)$, then $V_i(t) = 1$ and the site i is vacant. However, if one of the variables $p_i(t)$, $n_i^A(t)$, $n_i^B(t)$ is unity (note that at most *only one* atom can be present at location i at any time t), then the vacancy is absent at location i and hence $V_i(t) = 0$.

As in I, it is convenient to work with occupancy fluctuation variables. For the AB system there are two such variables

$$\mu_i(t) = n_i^{\mu}(t) - x_{\mu}, \quad \mu \equiv A,B . \tag{2.3}$$

Because x_{μ} is the atomic concentration of species μ,

$$\langle \mu_i(t) \rangle = 0 \tag{2.4a}$$

and

$$\langle V_i(t) \rangle = v = 1 - x_A - x_B , \tag{2.4b}$$

and Eqs. (2.1) can be recast into the following useful form:

$$\frac{dp_i}{dt} = -v \sum_j J_{ij}^0 (p_i - p_j) + \sum_{\mu=A,B} \sum_j J_{ij}^{\mu}(p_i \mu_j - p_j \mu_i) , \tag{2.5a}$$

$$\frac{dA_i}{dt} = -(1 - x_B) \sum_j J_{ij}^A (A_i - A_j) - x_A \sum_j J_{ij}^A (p_i - p_j) - \sum_i J_{ij}^A [p_i A_j - p_j A_i + x_A (B_i - B_j) + (A_j B_i - A_i B_j)] . \tag{2.5b}$$

[The corresponding equation for dB_i/dt can be obtained by inspection from (2.5b) by interchanging letters A and B.] The frequency Fourier transform of the equation of motion of the tracer occupancy Green's function is conveniently represented as follows:

$$\omega G_{gg'} = \delta_{gg'} - iv \sum_j J_{gj}^0 (G_{gg'} - G_{jg'}) + i \sum_{\mu=A,B} \sum_j J_{gj}^0 (G_{gj;g'}^{\mu} - G_{jg;g'}^{\mu}) . \tag{2.6}$$

In the above we introduced the notation

$$G_{gg'}(t) = -2\pi i \Theta(t) \langle p_g(t) p_{g'}(0) \rangle \equiv \langle\langle p_g(t); p_{g'}(0) \rangle\rangle = \int_{-\infty}^{+\infty} G_{gg'} \exp(-i\omega t) d\omega , \tag{2.7a}$$

$$G_{lj;g'}^{\mu}(t) = \langle\langle p_l(t) \mu_j(t); p_{g'}(0) \rangle\rangle, \quad \mu \equiv A,B = \int_{-\infty}^{+\infty} G_{lj;g'}^{\mu} \exp(-i\omega t) d\omega . \tag{2.7b}$$

As in I, it is convenient to work in terms of the inverse-lattice representation such that

$$G_{gg'} = \frac{1}{N} \sum_{\vec{K}} G_K \exp[i\vec{K} \cdot (\vec{g} - \vec{g}')] ,$$

$$G_{lj;g'}^{\mu} = \left[\frac{1}{N} \right]^2 \sum_{\vec{K}_1} \sum_{\vec{K}_2} G_{K_1,K_2}^{\mu} \exp[i\vec{K}_1 \cdot (\vec{l} - \vec{g}') + i\vec{K}_2 \cdot (\vec{j} - \vec{g}')] . \tag{2.8}$$

Equation (2.6) can now be written in a compact form that will be found most useful for the present treatment:

$$(\omega + iv\omega_K^0) G_K - 1 = iT(K,\omega) G_K , \tag{2.9a}$$

where

$$T(\vec{K},\omega) = J^0 \sum_{\vec{\delta}} [1 - \exp(i\vec{K} \cdot \vec{\delta})] \times [f^A(\vec{\delta}) + f^B(\vec{\delta})] , \tag{2.9b}$$

$$\omega_K^{\sigma} = J^{\sigma} z (1 - \gamma_K), \quad \sigma \equiv A,B,0 \tag{2.10a}$$

$$\gamma_K = \frac{1}{z} \sum_{\vec{\delta}} \exp(i\vec{K} \cdot \vec{\delta}) , \tag{2.10b}$$

$$f^{\mu}(\vec{\delta}) = \frac{1}{N} \sum_{\vec{\lambda}} G_{\vec{K} - \vec{\lambda}, \vec{\lambda}}^{\mu} \exp(-i\vec{\lambda} - \vec{\delta}) / G_K . \tag{2.11}$$

[For brevity, dependence of $f^{\mu}(\vec{\delta})$ on ω and $\vec{K}$ is not indicated.] If the scattering terms on the right-hand side of Eq. (2.9a) are ignored in comparison with those on the left-hand side, we get

$$(\omega+iv\omega_K^0)G_K-1\approx 0\ . \tag{2.12}$$

This is the well-known mean-field approximation (MFA). Thus the terms on the right-hand side, proportional to $f^{\mu}(\vec{\delta})$, represent the additional fluctuations from the MFA.

To treat these fluctuations adequately, it is necessary to examine the equation of motion of the two-particle Green's function G^{μ}. After some algebra, we find

$$\begin{aligned}\omega G^A_{lj;g'} = {} & x_A\{i(J^0_{lj}v+J^A_{lj})-[\omega+iz(J^0v+J^A)]\delta_{lj}\}G_{lg'} \\ & +iG^A_{lj;g'}\{(v-x_A)J^0_{lj}+J^A_{lj}(1-x_B)-z[J^0v+J^A(1-x_B)]\} \\ & +iG^B_{lj;g'}x_A(J^A_{lj}-J^0_{lj}-J^Az)+ix_AJ^0_{lj}(G^A_{jl;g'}+G^B_{jl;g'}) \\ & +i(1-\delta_{lj})\sum_i[x_AJ^A_{ji}G^B_{li;g'}+vJ^0_{li}G^A_{ij;g'}+(1-x_B)J^A_{ji}G^A_{li;g'}]+iR_{lj;g'}\ ,\end{aligned} \tag{2.13}$$

where

$$R_{lj;g'}=\sum_i J^0_{li}\Delta_{lj}\Delta_{ij}\langle\langle(p_lA_i-p_iA_l+p_lB_i-p_iB_l)A_j;p_{g'}\rangle\rangle+\sum_i J^A_{ij}\Delta_{lj}\Delta_{il}\langle\langle p_l(A_jB_i-A_iB_j);p_{g'}\rangle\rangle \tag{2.14a}$$

and

$$\Delta_{ij}\equiv 1-\delta_{ij}\ . \tag{2.14b}$$

Equation (2.13) is exact. However, the terms indicated by $R_{lj;g'}$ represent higher-order fluctuations. They involve, in addition to the tracer variable p, at least two additional renormalized particle fields—all at different locations. As explained in I, we expect these fluctuations to be $O(x_{\mu}v(1-v)(1-x_{\mu}))$ and $O(x_Ax_B(1-x_A)(1-x_B))$. Accordingly, in the small concentration limit, i.e., when $x_{\mu}\ll 1$, or x_A and $v\ll 0$ (or x_B and $v\ll 0$), the neglect of R terms is rigorously justified. On the other hand, while in the intermediate-concentration regime R is not vanishingly small, it is, nonetheless, smaller than the MFA terms which are of order v. As a reasonable approximation, therefore, in what follows the remainder R will be neglected.

III. SOLUTION

An inverse-lattice Fourier transform of (2.13) involves a set of coupled integral equations which give $G^A_{K_1,K_2}$ in terms of $G_{\vec{K}_1+\vec{K}_2}$, $G^B_{K_1,K_2}$, and sums of the form

$$\begin{aligned}I^{\mu}_1 &= \frac{1}{N}\sum_{\vec{\lambda}}\gamma_{\lambda}G^{\mu}_{\vec{K}_1-\vec{\lambda},\vec{K}_2+\vec{\lambda}}\ , \\ I^{\mu}_2 &= \frac{1}{N}\sum_{\vec{\lambda}}\gamma_{\lambda}G^{\mu}_{\vec{K}_2+\vec{\lambda},\vec{K}_1-\vec{\lambda}}\ , \\ I^{\mu}_3 &= \frac{1}{N}\sum_{\vec{\lambda}}\gamma_{\lambda}G^{\mu}_{\vec{K}_1+\vec{K}_2+\vec{\lambda},-\vec{\lambda}}\ .\end{aligned} \tag{3.1}$$

For general $\vec{K}_1$ and $\vec{K}_2$, exact solution of these equations seems nearly impossible to obtain. It turns out, however, that as in I an appropriate integral of these equations makes it possible to relate $f^{\mu}(\vec{\delta})$'s to themselves, thus providing us with a set of $2z$ linear equations for the $2z$ unknowns $f^{\mu}(\vec{\delta})$. Some of the essential manipulations are similar to those carried out in I, although the notation is different and many details of the algebra are more cumbersome. The result can be presented in the following form:

$$\begin{aligned}f^A(\vec{\delta}) &= \Phi^A(\vec{\delta})+\sum_{\vec{\delta}'}[L^A(\vec{\delta},\vec{\delta}')f^A(\vec{\delta}')+x_AM^A(\vec{\delta},\vec{\delta}')f^B(\vec{\delta}')]\ , \\ f^B(\vec{\delta}) &= \Phi^B(\vec{\delta})+\sum_{\vec{\delta}'}[L^B(\vec{\delta},\vec{\delta}')f^B(\vec{\delta}')+x_BM^B(\vec{\delta},\vec{\delta}')f^A(\vec{\delta}')]\ ,\end{aligned} \tag{3.2}$$

where

$$\Phi^A(\vec{\delta})=\frac{1}{N}\sum_{\vec{\lambda}}\exp(-i\vec{\lambda}\cdot\vec{\delta})N^A(\lambda)/D(\lambda)\ , \tag{3.3a}$$

$$N^A(\lambda)=-x_A\{\omega+i[v\omega^0_{\vec{K}-\vec{\lambda}}+(1-x_A)\omega^B_{\lambda}]\}[\omega+i(\omega^0_{\lambda}v+\omega^A_{\lambda})]+ix_Ax_B\omega^A_{\lambda}[\omega+i(v\omega^0_{\lambda}+\omega^B_{\lambda})]\ , \tag{3.3b}$$

$$D(\lambda)=\{\omega+i[v\omega^0_{\vec{K}-\vec{\lambda}}+(1-x_B)\omega^A_\lambda]\}\{\omega+i[v\omega^0_{\vec{K}-\vec{\lambda}}+(1-x_A)\omega^B_\lambda]\}+x_Ax_B\omega^A_\lambda\omega^B_\lambda\,, \tag{3.3c}$$

and

$$\begin{aligned}L^A(\vec{\delta},\vec{\delta}')=&[(v-x_A)J^0+J^A(1-x_B)]P^A(\vec{\delta}-\vec{\delta}')+x_AJ^0\exp(i\vec{K}\cdot\vec{\delta}')P^A(\vec{\delta}+\vec{\delta}')\\&-[vJ^0\exp(i\vec{K}\cdot\vec{\delta}')+(1-x_B)J^A]P^A(\vec{\delta})\\&+x_Ax_B[(J^B-J^0)Q^A(\vec{\delta}-\vec{\delta}')+J^0\exp(i\vec{K}\cdot\vec{\delta}')Q^A(\vec{\delta}+\vec{\delta}')-J^BQ^A(\vec{\delta})]\,,\end{aligned} \tag{3.4}$$

$$\begin{aligned}M^A(\vec{\delta},\vec{\delta}')=&(J^A-J^0)P^A(\vec{\delta}-\vec{\delta}')+J^0\exp(i\vec{K}\cdot\vec{\delta}')P^A(\vec{\delta}+\vec{\delta}')-J^AP^A(\vec{\delta})\\&+[(v-x_B)J^0+J^B(1-x_A)]Q^A(\vec{\delta}-\vec{\delta}')+x_BJ^0\exp(i\vec{K}\cdot\vec{\delta}')Q^A(\vec{\delta}+\vec{\delta}')\\&-[vJ^0\exp(i\vec{K}\cdot\vec{\delta}')+(1-x_A)J^B]Q^A(\vec{\delta})\,.\end{aligned} \tag{3.5}$$

The quantities $P^\mu(\vec{r})$ and $Q^\mu(\vec{r})$ are related to the generalized Watson sums that depend on both ω and $\vec{K}$:

$$P^A(\vec{r})=\frac{i}{N}\sum_{\vec{\lambda}}\exp(-i\vec{\lambda}\cdot\vec{r})\{\omega+i[v\omega^0_{K-\lambda}+(1-x_A)\omega^B_\lambda]\}/D(\lambda)\,, \tag{3.6a}$$

$$Q^A(\vec{r})=\frac{1}{N}\sum_{\vec{\lambda}}\exp(-i\vec{\lambda}\cdot\vec{r})\omega^A_\lambda/D(\lambda)\,. \tag{3.6b}$$

Once the quantities $f^\mu(\vec{\delta})$ have been obtained, the mass operator of the Green's function is readily found, i.e.,

$$G_K=[\omega+iv\omega^0_KF(\vec{K},\omega)]^{-1}\,, \tag{3.7a}$$

where

$$F(\vec{K},\omega)=1-T(\vec{K},\omega)/(v\omega^0_K)\,. \tag{3.7b}$$

[Note $T(K,\omega)$ depends on a simple sum of $f^\mu(\vec{\delta})$'s as given in Eq. (2.9b). Also note that $\Phi^B(\vec{\delta})$, $L^B(\vec{\delta},\vec{\delta}')$, and $M^B(\delta,\vec{\delta}')$ need not be given explicitly since the relevant expressions can be readily found from those for $\Phi^A(\vec{\delta})$, $L^A(\vec{\delta},\vec{\delta}')$, and $M^A(\vec{\delta},\vec{\delta}')$.]

IV. RESULTS

Coefficients of the $2z$ coupled linear equations (3.2) for the $2z$ unknowns $f^\mu(\vec{\delta})$ involve inverse lattice sums $\Phi^\mu(\vec{\delta})$, $P^\mu(\delta)$, $Q^\mu(\vec{\delta})$, $P^\mu(\vec{\delta}\pm\vec{\delta})$, and $Q^\mu(\delta\pm\vec{\delta}')$. While these sums are straightforward to do on the computer, for arbitrary $\vec{K}$ directions they can involve tedious computation. For example, for general $\vec{K}$, the relevant sums over the Brillouin zone retain none of the 48-fold cubic symmetry that the $\vec{K}$-independent Watson sums possess. Moreover, for such $\vec{K}$'s the number of sums needed is of order $3z+2z^2$. In contrast, for $\vec{K}$ values along high-symmetry directions, it is usually possible to reduce the $2z$ equations to a small number, such as 4 or 6, etc., and equally importantly it is possible also to exploit the symmetry property of the Brillouin zone. Together, these simplifications can result in reducing the computer time by as much as 2 orders of magnitude; namely, to the order of a few minutes rather than many hours.

Another important feature of Eqs. (3.2)–(3.6b) is the freedom from any requirement for dynamical self-consistency. Self-consistency, even when it is rigorously assured, can increase computational effort by an order of magnitude and, worse still, is at times quite unachievable (compare, for instance, certain types of coherent potential approximations[18]).

For small $\vec{K}$ and small frequency ω, these equations can, however, be solved analytically. This yields the well-known diffusive limit, for which

$$F(\vec{K},\omega)\underset{\substack{J^0K^2\ll\omega,\\ \omega\ll J^0z}}{\longrightarrow}f_0\,. \tag{4.1}$$

The correlation factor f_0 is found to be given as follows:

$$f_0^{-1}=1-\frac{2J^0\langle\cos\theta\rangle\rho_0}{\nu_0(1+\langle\cos\theta\rangle)}\,, \tag{4.2}$$

$$\begin{aligned}\rho_0=&vJ^0(x_A+x_B)+x_A(1-x_A)J^B\\&+x_B(1-x_B)J^A-x_Ax_B(J^A+J^B)\,,\\ \nu_0=&[vJ^0+(1-x_B)J^A][vJ^0+(1-x_A)J^B]\\&-x_Ax_BJ^AJ^B\,.\end{aligned} \tag{4.3}$$

Quantity $\langle\cos\theta\rangle$ depends only on the lattice structure and is well known for a variety of three-dimensional lattices [see for example, Eq. I(3.18)]. For two-dimensional square lattice we have computed it to be approximately equal to -0.3634, whereas in one dimension it is equal to -1 and hence $f_0=0$.

It should be noted that Eq. (4.2) reduces to the corresponding result for a single-component system with vacancy concentration v whenever $J^A=J^B=J$ [to compare this with Eq. I(3.19), use the fact that

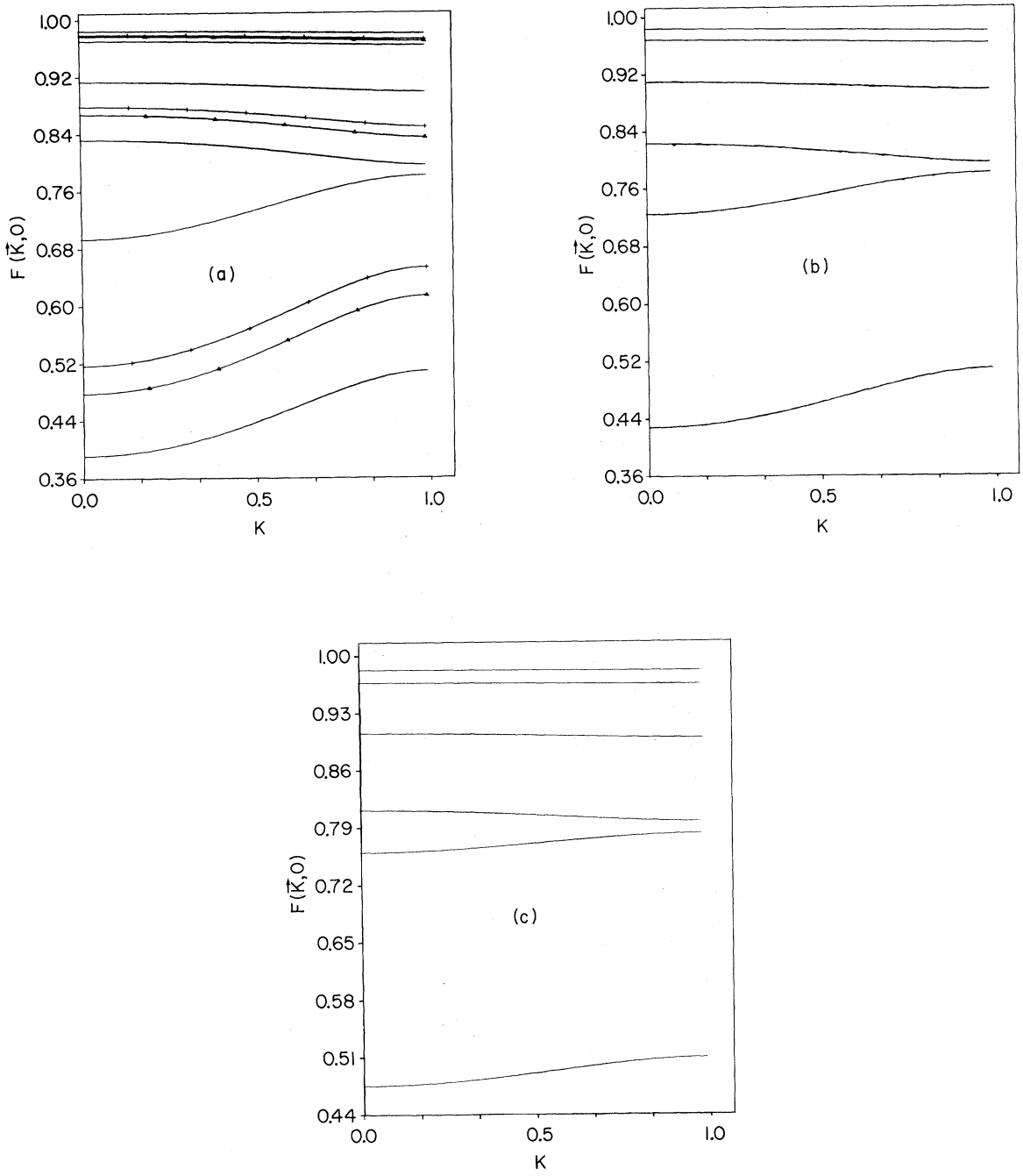

FIG. 1. (a) $F(\vec{K},0)$ is plotted as a function of K for $\vec{K}=\pi(K,K,K)$. There are three sets of curves, each consisting of two continuous curves—one at the top and one at the bottom of each set—and two other curves, the upper of which has $+$ signs and the lower one has small triangles. The uppermost set of four curves refers to the case $v=0.9$, the middle set to $v=0.5$, and the lowest set to $v=0.001$. The top and the bottom continuous curves in each set are for $\eta=4$ and $\frac{1}{4}$, respectively, while the curves with plus signs relate to $\eta=1$ and the ones with triangles to $\eta=1/\sqrt{2}$. (b) $F(\vec{K},0)$ vs K for $\vec{K}=\pi(K,K,0)$. Otherwise, the figure is similar to (a) with the only difference that the curves for $\eta=1$ and $\eta=1/\sqrt{2}$ (which has $+$ signs and triangles, respectively) are omitted. (c) Same as for (b) with the only difference that now $\vec{K}=\pi(K,0,0)$.

TABLE I. To compare our estimate for the diffusion coefficient, or equivalently the tracer correlation factor f_0 given in Eqs. (4.2) and (4.3), with that of Manning (Ref. 4), we show here the case where the tracer is identical to A atoms (hydrogen, for example), and the background consists of a mixture of x_A (hydrogen atoms) and $x_B=1-x_A$, deuterium atoms. The hopping rates have been assumed to have the ratio given in (4.5), i.e., $J^A/J^B=\sqrt{2}$. The columns labeled f_0 give the results of the present paper whereas the columns marked "ratio" represent the ratio of Manning's f_0 to our f_0.

	Simple cubic		Face-centered cubic	
A	f_0	Ratio	f_0	Ratio
1.00	0.653 11	1.00 00	0.781 45	1.00 00
0.90	0.645 63	1.00 05	0.776 00	1.00 06
0.80	0.637 97	1.00 10	0.770 34	1.00 10
0.70	0.630 14	1.00 12	0.764 46	1.00 15
0.60	0.622 14	1.00 13	0.758 35	1.00 17
0.50	0.613 97	1.00 13	0.752 00	1.00 18
0.40	0.605 66	1.00 12	0.745 41	1.00 17
0.30	0.597 19	1.00 10	0.738 58	1.00 15
0.20	0.588 60	1.00 07	0.731 50	1.00 12
0.10	0.579 88	1.00 04	0.724 17	1.00 07
0.00	0.571 06	1.00 00	0.716 58	1.00 00

here $x_A+x_B=1-v=x$ of paper I]. Moreover, when either x_A or x_B is vanishing, the above result once again reduces to that given in I(3.19).

Another feature of the result (4.2) worth noticing is that we do not expect it to be reliable when either J^A or J^B, or both J^A and J^B, lie outside the range $zJ^0>J^\lambda>J^0/z$. This is in contrast to paper I where the validity of the theory was restricted only to the case where $J>J^0/z$. The reason is that here the relevant fluctuations are proportional to J^0 as well as J^A and J^B, which are being neglected [compare the remainder (2.14a) and the one referring to paper I, the latter being proportional only to J^0]. In three dimensions this restriction is not a serious one in practice, but it would be useful to have a theory which is reliable throughout the range $0\leq J^\lambda/J^0\leq\infty$. In order to give a feeling for the accuracy of the theory for only moderately different hopping rates, in Table I we append a comparison of the present results with those given by Manning's calculation for the case of hydrogen atom diffusion in a hydrogen-deuterium mixture where the vacancy concentration is vanishing. (Note Manning's work is restricted to the case of zero vacancy concentration.) We find that the two sets of predictions differ by at most two parts in a thousand and this occurs near the worst possible point of 50-50 concentration of hydrogen and deuterium.

At general $\vec{K}$ and ω, we study a case that cannot be treated adequately within the restricted format of I. This happens when the concentrations, x_A and x_B, of both the components are finite. For brevity, however, in all the discussion that follows we consider only the equiconcentration case, i.e.,

$$1-v=2x_A=2x_B=C\ . \tag{4.4}$$

Also for brevity we consider the tracer to be identical to the A variety of atoms (say, hydrogen) so that $J^0=J^A$. Now, after setting the frequency scale, by

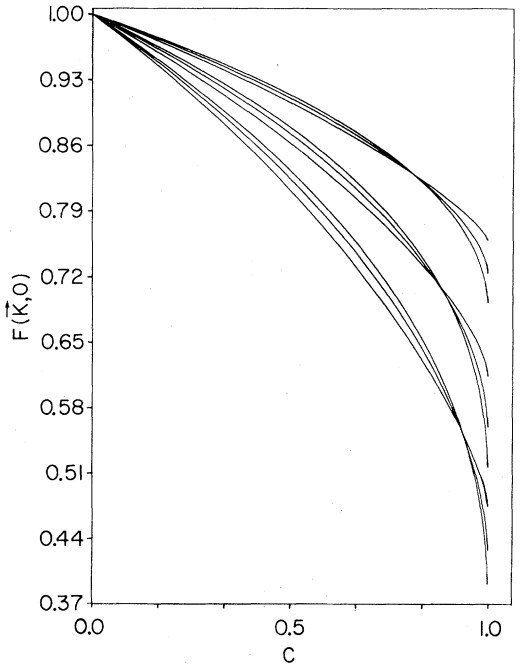

FIG. 2. $F(\vec{K},0)$ is plotted vs $(1-v)=C$. The top set of three curves is for $\eta=4$, the middle set for $\eta=1$, and the lowest set for $\eta=\frac{1}{4}$. For each of the sets, the highest curve at $C=1$ refers to $\vec{K}=\pi(1,0,0)$, the middle one to $\vec{K}=\pi(1,1,0)$, and the lowest one to $\vec{K}=\pi(1,1,1)$.

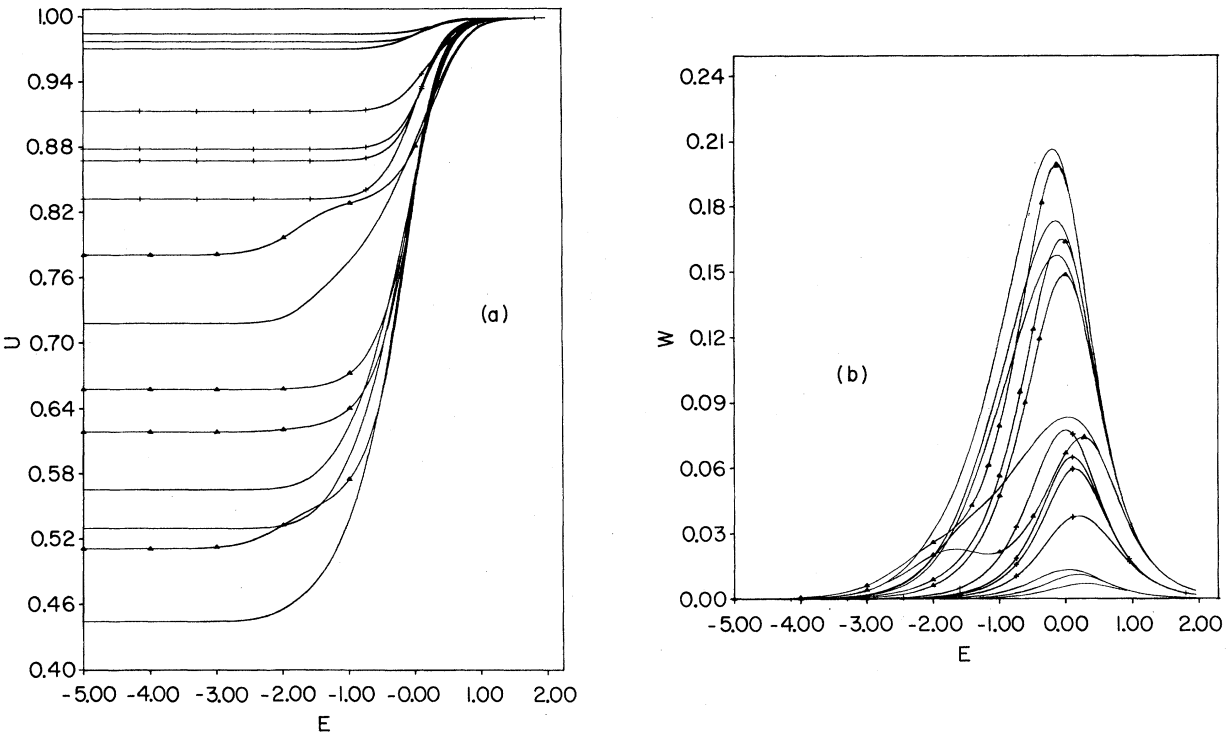

FIG. 3. (a) Real part U of the generalized correlation factor $F(\vec{K},\omega)$ is given as a function of E. The curves are identified in decreasing order of their heights at $E=-5$ as follows: For the top three continuous curves, $v=0.9$ and $\eta=4$, 1, and $\frac{1}{4}$, in decreasing order of heights, respectively. For the next lower set of four curves with + signs, $\eta=4$, 1, $1/\sqrt{2}$, and $\frac{1}{4}$, respectively, and $v=0.5$. The $\vec{K}$ value for these top seven curves is equal to $\pi(1,1,1)$. The eight remaining curves refer to $v=0.01$. These fall into two sets of four curves each. The set with small triangles refers to $\vec{K}=(0,0,0)$. In decreasing order of heights (at $E=-5$) the curves for this set refer to $\eta=4$, 1, $1/\sqrt{2}$, and $\frac{1}{4}$, respectively. The remaining set of four curves (without any markings) are for $\vec{K}=\pi(1,1,1)$ and in decreasing order of heights (at $E=-5$) they too represent the cases $\eta=4$, 1, $1/\sqrt{2}$, and 4, respectively. (b) Negative imaginary part W of the generalized correlation factor is plotted as a function of E. The curves can be readily identified by comparing with (a). The maximum peak heights in this figure correspond to minimum values for U at $E=-5$. Thus the highest peak in this figure refers to $\eta=\frac{1}{4}$, $v=0.01$, and $\vec{K}=\pi(1,1,1)$.

setting $zJ^A=1$, the ratio $\eta=J^B/J^A$ needs to be specified. To this end we invoke an assumption that should be adequate for most purposes, at least qualitatively: that is, the classical isotope effect obtains[19–22]

$$\eta=J^B/J^A=(m^A/m^B)^{1/2}\,, \tag{4.5}$$

where m^A is the atomic mass of component A.

As noted in I, correlation effects on the hopping motion of the tracer are most noticeable after protracted motion. Within the Fourier transformed representation, this corresponds to

$$\omega \ll 1\,. \tag{4.6}$$

(For simplicity and brevity, all the succeeding analysis is limited to the case of a simple cubic lattice with unit elementary cube edge length. Moreover, to represent a system with hydrogen-deuterium mixture, we choose both the tracer and the component A atoms to be hydrogen and component B to be deuterium.)

The generalized correlation factor $F(\vec{K},\omega)$ is shown for $\omega=0$, in Figs. 1 and 2, as a function of the wave vector $\vec{K}$ and the particle concentration C. We observe that for $x_A=x_B=C/2=5\%$, i.e., $v=0.9$, the changes in $F(\vec{K},0)$ caused by altering the composition of the background from equal concentration of hydrogen and deuterium to a case where the background is composed only of hydrogen are barely noticeable to an unaided eye. In contrast, the corresponding two sets of results begin to differ appreciably when vacancy concentration is reduced down to about 50%. Indeed, for the small vacancy

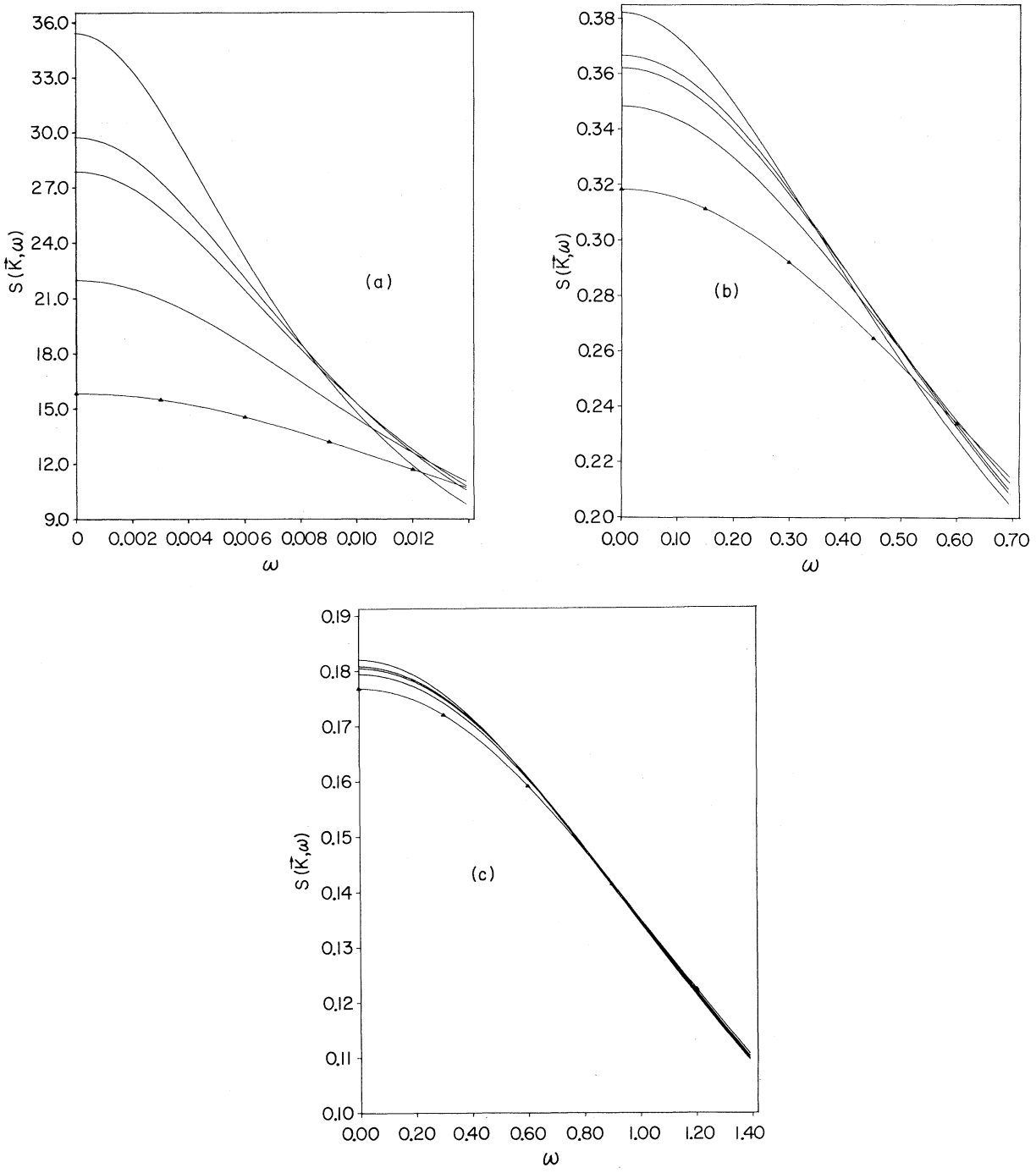

FIG. 4. (a) Incoherent response $S(\vec{K},\omega)$ is given as a function of ω. Here $\vec{K}=\pi(1,1,1)$ and $v=0.01$. The top four curves, according to decreasing order of heights at zero frequency, are for $\eta=\frac{1}{4}$, $1/\sqrt{2}$, 1, and 4, respectively. The bottom curve (with triangles) represents the MFA result for all η. (b) Same as (a) for $v=0.5$. (c) Same as (a) for $v=0.9$.

limit [e.g., $v=0.001$ shown in Figs. 1(a)–1(c)] the composition of the background makes a substantial difference in the results. Note that the correlation effects become more prominent with increase in the deuterium concentration.

To investigate both the $\vec{K}$ and ω dependence of $F(\vec{K},\omega)$, it is convenient to look at its real and imaginary parts separately. We have

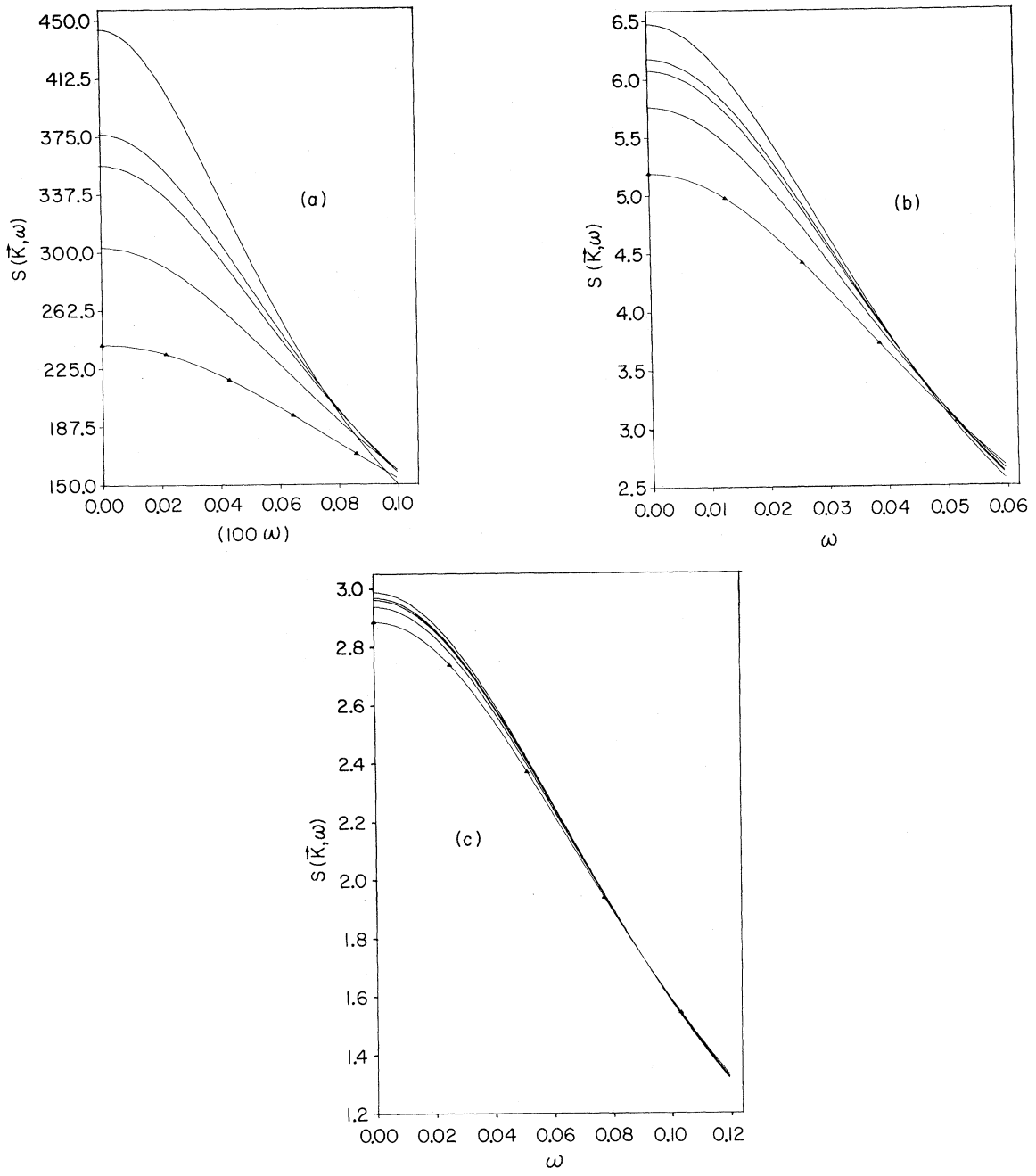

FIG. 5. These figures correspond to Figs. 4(a)—4(c), respectively, with the only difference that here $\vec{K}=0.5(1,1,1)$.

$$\lim_{\epsilon\to 0+} F(K,\omega+i\epsilon)=U-iW\ . \tag{4.7}$$

In Figs. 3(a) and 3(b), the real, U, and the negative imaginary, W, parts are plotted for a variety of values of $\vec{K}$, η, and the vacancy concentration, v. For convenience, these are given as functions of E where

$$E=\log_{10}\omega\ . \tag{4.8}$$

Both the real and the imaginary parts of the generalized correlation factor are observed to be smooth functions of E, the latter displaying a single peak. Only for small wave vectors do the curves for U contain a slight shoulder (this is reflected as a weak secondary maximum in W). Because the quantity

of experimental interest, referred to as the incoherent response function

$$S(\vec{K},\omega)=-(1/\pi)\mathrm{Im}G_K(\omega+i\epsilon),\quad \epsilon\to 0+ \qquad (4.7)$$

contains an ω^2 term in the denominator, the effects of such a shoulder are essentially masked for all the measurable wave vectors.

The above fact is demonstrated in Figs. 4 and 5, where we have plotted the response as a function of ω for both large $\vec{K}$ (i.e., at the zone boundary along the cube diagonal) and small $\vec{K}$ (i.e., about 16% of the way along the diagonal from the zone center). We observe, firstly, that the curves are completely smooth with no trace of a cusp at $\omega=0$. Secondly, the relative separation between the $\eta=(1/\sqrt{2})$ and $\eta=1$ curves (the former refers to the case where the background is half hydrogen and half deuterium, for example, while the latter refers to the background being all hydrogen) is a strong function of the vacancy concentration v (being most pronounced for small v) but only a weak function of $\vec{K}$.

Thus, in a neutron scattering experiment, the presence of deuterium background (instead of the hydrogen background) should be noticeable only as long as vacancy concentration is less than $\sim 90\%$. For $v\sim 50\%$, appreciably different results for the two types of backgrounds can be expected. In this connection it should be mentioned that for the system PdH_xD_y the relevant lattice is fcc. This acts to further reduce the observability of the differences between the hydrogen and the deuterium backgrounds, and for constant $C=x+y$ the results are somewhat insensitive to changes in x and y as long as $C\lesssim 0.1$. For $C\gtrsim 0.15$, however, the different blocking rates for different compositions of hydrogen and deuterium should affect the results for the response sufficiently strongly to be measured.

ACKNOWLEDGMENTS

This paper is an outgrowth of work originally started at University of Oxford with Professor R. J. Elliott (paper I). I am grateful to Professor Elliott for advice and discussion. I have also benefited from discussions with Professor K. Binder and Dr. K. W. Kehr and Dr. K. Schröder at Jülich. This work was in part carried out at the International Centre for Theoretical Physics (ICTP), Trieste, Italy. I am greatly indebted to Professor E. Tossatti for hospitality at ICTP. Part of the work was written up at the University of California, Santa Barbara. I am indebted to the Institute for Theoretical Physics, the Department of Physics, Professor J. R. Schrieffer, Professor Douglas Scalapino, Professor D. Hone, and Professor Vincent Jaccarino for hospitality. Financial support from the National Science Foundation, Grant No. DMR-80-13700, and a grant-in-aid of research from Temple University is gratefully acknowledged.

[1]R. A. Tahir-Kheli and R. J. Elliot, Phys. Rev. B 27, 844 (1983).

[2]J. Bardeen and C. Herring, in *Imperfections in Nearly Perfect Crystals,* edited by W. Shockley (Wiley, New York, 1952).

[3]A. D. LeClaire and A. B. Lidiard, Philos. Mag. 1, 518 (1956).

[4]J. R. Manning, Acta. Metallurg. 15, 817 (1967); *Diffusion Kinetics for Atoms in Crystals,* (Van Nostrand, Princeton, 1968); Phys. Rev. B 4, 1111 (1971).

[5]H. J. De Bruin, G. E. Murch, H. Bakker, and L. P. Van der Mey, Thin Solid Films 25, 47 (1975).

[6]G. E. Murch and S. J. Rothman, Philos. Mag. A43, 229 (1981).

[7]Y. Fukai, K. Kubo, and S. Kazama, Z. Phys. Chem. N.F. 115, 181 (1979); H. Sugimoto and Y. Fukai, Suppl. Trans. Jpn. Inst. of Metallurg. 21, 177 (1980); S. Kazama and Y. Fukai, *ibid.* 21, 173 (1980).

[8]R. Kutner and K. W. Kehr (unpublished).

[9]O. F. Sankey and P. A. Fedders, Phys. Rev. B 15, 3586 (1977); 20, 39 (1979); 22, 5135 (1980).

[10]P. M. Richards, Phys. Rev. B 16, 1393 (1977).

[11]P. A. Fedders, Phys. Rev. B 17, 40 (1978).

[12]S. Alexander and P. Pincus, Phys. Rev. B 18, 2011 (1978).

[13]K. W. Kehr, R. Kutner, and K. Binder, Phys. Rev. B 23, 4931 (1981).

[14]P. A. Fedders and O. F. Sankey, Phys. Rev. B 15, 3580 (1977); 18, 5938 (1978).

[15]K. W. Kehr, R. Kutner, and K. Binder (unpublished).

[16]J. Van Beijeren, K. W. Kehr, and R. Kutner (unpublished).

[17]K. Nakazato and K. Kitahara, Prog. Theor. Phys. 64, 2261 (1980).

[18]R. J. Elliott, J. Krumhansl, and P. L. Leath, Rev. Mod. Phys. 46, 465 (1974).

[19]J. G. Mullen, Phys. Rev. 121, 1649 (1961).

[20]H. R. Glyde, Phys. Rev. 180, 722 (1968).

[21]L. Katz, M. Guinan, and R. J. Borg, Phys. Rev. B 4, 330 (1971).

[22]For a comprehensive recent review, see J. Völkl and G. Alefeld, in *Hydrogen in Metals,* Vol. 28 of *Topics in Applied Physics,* edited by G. Alefeld and J. Völkl (Springer, New York, 1978).